



Gas-phase ion chemistry within the photodetachment-modulated electron capture detector
by Kyle Scott Strode

A thesis submitted in partial fulfillment of the requirements for the degree of Doctor of Philosophy in Chemistry

Montana State University

© Copyright by Kyle Scott Strode (1993)

Abstract:

The objective of this thesis is to expand the utility of the photodetachment-modulated electron capture detector (PDM-ECD) for the study of gas-phase ion chemistry (GPIC) at atmospheric pressure. Specifically, studies of electron photodetachment (PD), a unique electron capture (EC) reaction and two gas-phase ion-molecule reactions at atmospheric pressure are reported.

In the PDM-ECD, p-benzoquinone and its methylated derivatives undergo optical enhancement of EC (OEEC) during irradiation by ultraviolet light. The molecular anions of the quinones also undergo PD over the same wavelength range. A method is described in which the OEEC and PD spectra can be independently measured without interference from each other. The OEEC and PD spectra are reported and compared with solution-phase absorption spectra. From mass spectrometric experiments, the OEEC response is attributed to EC by photochemically produced dimers of the quinones.

By comparison of the PD spectra for I⁻ under dry conditions and with a few torr of water added to the detector gas, the onset for PD from I⁻(H₂O) is shown to occur at a photon energy greater than that for I⁻ by an amount equal to the enthalpy of solvation. The equilibrium constant for the clustering reaction is calculated at 130°C from comparisons of PD responses under dry and wet conditions.

It is shown that gas-phase S_N2 displacement will occur at atmospheric pressure in the PDM-ECD between an alkyl bromide (RBr) and Cl⁻. Chromatographic introduction of RBr is important for separating impurities from the compound of interest. The PD response to Br⁻ produced by the reaction is induced by 365 nm light from a Hg/Xe lamp. A method is shown whereby measuring the PD response at different concentrations of RBr gives information that can be used to determine the second-order rate constant for S_N2 displacement, K_{SN2}, between RBr and Cl⁻. The values for K_{SN2} are reported for 18 alkyl bromides and compared with previously reported gas- and solution-phase results. The temperature dependence of K_{SN2} from 100-200°C is reported for bromomethane and 2-bromopropane.

GAS-PHASE ION CHEMISTRY WITHIN
THE PHOTODETACHMENT-MODULATED
ELECTRON CAPTURE DETECTOR

by

Kyle Scott Strode

A thesis submitted in partial fulfillment
of the requirements for the degree

of

Doctor of Philosophy

in

Chemistry

MONTANA STATE UNIVERSITY
Bozeman, Montana

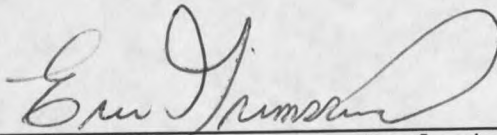
April 1993

D378
St872

APPROVAL
of a thesis submitted by
Kyle Scott Strode

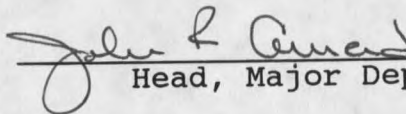
This thesis has been read by each member of the thesis committee and has been found to be satisfactory regarding content, English usage, format, citations, bibliographic style, and consistency, and is ready for submission to the College of Graduate Studies.

3/31/93
Date


Chairperson, Graduate Committee

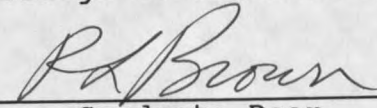
Approved for the Major Department

3-30-93
Date


Head, Major Department

Approved for the College of Graduate Studies

3/31/93
Date


Graduate Dean

STATEMENT OF PERMISSION TO USE

In presenting this thesis in partial fulfillment of the requirements for a doctoral degree at Montana State University, I agree that the Library shall make it available to borrowers under rules of the Library. I further agree that copying of this thesis is allowable only for scholarly purposes, consistent with "fair use" as prescribed in the U.S. Copyright Law. Requests for extensive copying or reproduction of this thesis should be referred to University Microfilms International, 300 North Zeeb Road, Ann Arbor, Michigan 48106, to whom I have granted "the exclusive right to reproduce and distribute my dissertation for sale in and from microform or electronic format, along with the right to reproduce and distribute my abstract in any format in whole or in part."

Signature Kyle Stroh
Date 3-31-93

ACKNOWLEDGEMENT

I would like to thank several past and present members of the research group, especially Dr. Berk Knighton, Dr. Joe Sears and Dr. Steve Mock. I am indebted to them for their helpful suggestions and assistance and for meaningful discussions of the chemistry reported here. I thank all of the members of the research group for help and advice along the way and especially for their friendship. I am grateful to my advisor, Dr. Eric Grimsrud, for his support of my research and for fostering an environment in which I gained a full and mature understanding of chemistry.

I thank my whole family for their moral support, especially my mom and dad for providing an inspiring scholastic example and for nurturing my interest in science. Lastly, I deeply thank Julie for her profound love and support.

TABLE OF CONTENTS

	Page
INTRODUCTION	1
Gas-Phase Ion Chemistry	1
The PDM-ECD	3
Use of the PDM-ECD for Studies of GPIC	7
THEORY	11
Collision Frequency and Thermalization Within the PDM-ECD	11
Reactions Within the Cell	12
Equilibrium Within the PDM-ECD	17
EXPERIMENTAL	19
The PDM-ECD Setup	19
The ECD	20
Sample Introduction	20
Calculation of Sample Concentration Within the PDM-ECD	22
Doping of the Make-Up Gas	23
Optical System	27
Signal Processing	29
Measurement of PD Spectra	32
Setup of the APIMS	32
Ion Source	34
Optical System	34
Quadrupole	35
Sample Introduction	35
RESULTS AND DISCUSSION	36
Gas-Phase Photochemistry of Quinone Molecules and Their Molecular Anions	36
Description of the Problem	37
Characterization of OEEC Using the PDM-ECD	39
Temperature Dependence of EC Response	40
Lack of OEEC for $C_{12}H_{26}$ and $C_{18}H_{38}$	42
Dependence of OEEC on Concentration	43
Characterization of OEEC Using a Chopped Light Beam	46
Method For Independent Measurement of OEEC and PD	55

TABLE OF CONTENTS-Continued

	Page
PD Spectra of the Quinone Molecular Anions	57
Direct Photodetachment	59
Resonance Photodetachment	62
OEEC Spectra of the Quinones	64
Characterization of OEEC Using APIMS	68
Elucidation of the Mechanism	
Responsible for OEEC	74
Possible Structures of the Dimers	81
PDM-ECD Study of Iodide-Water	
Clustering Equilibria	83
Response of PDM-ECD to Iodide	
With Water Present	84
Relative Abundances of Iodide-Water Clusters	
From PDM-ECD Measurements	87
Determination of Equilibrium Constants and	
Thermochemical Data for the Iodide-Water	
Clustering Reaction	90
Comparison of the PD Spectra of I^-	
Under Dry and Wet Conditions	91
Determination of ΔH From PD Spectra	94
Kinetics of Gas-Phase S_N2 Reactions of	
Alkyl Bromides With Chloride	95
Introduction of Reactants and Monitoring	
of S_N2 Displacement	97
Experimental Measurement of S_N2 Displacement	99
Derivation of S_N2 Rate Law	103
Procedure for Measurement	
of S_N2 Rate Constants	105
Results of Rate Constant Measurements	107
Saturated Alkyl Bromides	108
Unsaturated Compounds	123
Temperature Dependence of S_N2 Rate Constants	126
SUMMARY	130
LITERATURE CITED	137

LIST OF TABLES

Table	Page
1. Photodetachment thresholds of the quinone anions .	60
2. EC rate coefficients for the quinone molecules . .	81
3. Rate constants and relative reactivities for RBr + Cl ⁻ ---> RCl + Br ⁻	112
4. Rate constants for reactions of BM and 2BPR with Cl ⁻ from 100° to 200°	128
5. Values from Arrhenius plots of rate constants for reactions of bromomethane and 2-bromopropane with Cl ⁻	128

LIST OF FIGURES

Figure	Page
1. Apparatus used for the PDM-ECD studies	19
2. Gaussian peak model used for calculation of sample concentration within the ECD	24
3. Configuration of the make-up gas line to allow for addition of dopants to the cell	26
4. Emission spectra of the Xe and Hg/Xe arc lamps	28
5. Circuit diagram for the pulser and electrometer used for the PDM-ECD	30
6. Apparatus used for APIMS studies	33
7. Electron capture detector responses to 200 ng of 200 ng of <i>p</i> -benzoquinone through repeated GC analyses of a standard solution while varying the conditions of the cell irradiation	38
8. Electron capture detector responses to 200 ng of <i>p</i> -benzoquinone through repeated GC analyses while varying the temperature of the cell without irradiation	41
9. Response of the PDM-ECD to varying concentrations of <i>p</i> -benzoquinone with and without irradiation	44
10. Response enhancement of the PDM-ECD observed with light of 240 nm and at varying concentrations of <i>p</i> -benzoquinone	45
11. GC analysis of <i>p</i> -benzoquinone with chart paper speed of 1 cm sec ⁻¹ and with 240 nm light chopped at 0.5 Hz	48
12. Graph used to calculate the time constant for the rate of change of the chemical system within the ECD at three different flow rates	51
13. Simulation of the two waveforms sent to the lock-in amplifier and the phase angle offset used to achieve the maximum negative output	54
14. Electron photodetachment spectra of the quinone molecular anions	58

LIST OF FIGURES-Continued

Figure	Page
15. Optically enhanced electron capture spectra of the quinones	66
16. Condensed-phase absorption spectra of the quinone molecules	67
17. Negative ion atmospheric pressure ionization mass spectra of <i>p</i> -benzoquinone with and without irradiation by 240 nm light	71
18. Superimposed single ion chromatograms for $m/z = 108$ and $m/z = 216$ from APIMS	72
19. Negative ion atmospheric pressure ionization mass spectra of <i>p</i> -benzoquinone recorded before and after abruptly extinguishing the light	73
20. Possible structures of the dimers of <i>p</i> -benzoquinone and 2,6-dimethyl- <i>p</i> -benzoquinone	82
21. PDM-ECD chromatograms of CH_3I with and without 3.9 torr water at 130°C and with 380 nm light	85
22. Relative abundances in the PDM-ECD of I^- and $\text{I}^-(\text{H}_2\text{O})_n$ from 130 - 190°C with 3.9 torr water present in the detector gas	89
23. Electron photodetachment spectra of I^- at 100°C under dry conditions and with 1.9 torr water present in the detector gas	92
24. Response of the PDM-ECD to 1-bromobutane chromatographically introduced to the detector with Cl^- continuously present	100
25. Plot of the magnitudes of $\text{S}_{\text{N}}2$ responses as a function of the concentration of bromoethane in the detector at the peak maxima	102
26. Response of the PDM-ECD to different concentrations of 1-bromobutane with Cl_- present	106
27. Plots of ECD concentrations of RBr vs. $[\text{Br}^-]/[\text{Cl}^-]$ for six primary unsubstituted saturated alkyl bromides	109

LIST OF FIGURES-Continued

Figure		page
28.	Plots of ECD concentrations of RBr vs. $[\text{Br}^-]/[\text{Cl}^-]$ for three primary substituted and three secondary saturated alkyl bromides	110
29.	Plots of ECD concentrations of RBr vs. $[\text{Br}^-]/[\text{Cl}^-]$ for six primary unsaturated alkyl bromides	111
30.	Reaction coordinate for the $\text{S}_{\text{N}}2$ displacement reaction of Cl^- with RBr where $\text{R} = \text{CH}_3$	117
31.	Arrhenius plots of rate constants for bromomethane and 2-bromopropane between 100 and 200°C	129

ABSTRACT

The objective of this thesis is to expand the utility of the photodetachment-modulated electron capture detector (PDM-ECD) for the study of gas-phase ion chemistry (GPIC) at atmospheric pressure. Specifically, studies of electron photodetachment (PD), a unique electron capture (EC) reaction and two gas-phase ion-molecule reactions at atmospheric pressure are reported.

In the PDM-ECD, *p*-benzoquinone and its methylated derivatives undergo optical enhancement of EC (OEEC) during irradiation by ultraviolet light. The molecular anions of the quinones also undergo PD over the same wavelength range. A method is described in which the OEEC and PD spectra can be independently measured without interference from each other. The OEEC and PD spectra are reported and compared with solution-phase absorption spectra. From mass spectrometric experiments, the OEEC response is attributed to EC by photochemically produced dimers of the quinones.

By comparison of the PD spectra for I^- under dry conditions and with a few torr of water added to the detector gas, the onset for PD from $I^-(H_2O)$ is shown to occur at a photon energy greater than that for I^- by an amount equal to the enthalpy of solvation. The equilibrium constant for the clustering reaction is calculated at 130°C from comparisons of PD responses under dry and wet conditions.

It is shown that gas-phase S_N2 displacement will occur at atmospheric pressure in the PDM-ECD between an alkyl bromide (RBr) and Cl^- . Chromatographic introduction of RBr is important for separating impurities from the compound of interest. The PD response to Br^- produced by the reaction is induced by 365 nm light from a Hg/Xe lamp. A method is shown whereby measuring the PD response at different concentrations of RBr gives information that can be used to determine the second-order rate constant for S_N2 displacement, k_{SN2} , between RBr and Cl^- . The values for k_{SN2} are reported for 18 alkyl bromides and compared with previously reported gas- and solution-phase results. The temperature dependence of k_{SN2} from 100-200°C is reported for bromomethane and 2-bromopropane.

INTRODUCTION

Gas-Phase Ion Chemistry

In the 1960's, mass spectrometric methods were developed which allowed scientists to study the behavior of ions in the gas phase under controlled conditions. Although ions are produced and controlled easily in the condensed phase, the electrostatic interactions with the solvent often have a pronounced effect on the dynamics, energetics and mechanism of an ionic reaction (1). In the gas phase, the presence of solvent can be eliminated or carefully controlled, and the intrinsic properties of ions and molecules can be studied (2). During the last 30 years, research in gas-phase ion chemistry (GPIC) has had a profound impact on a wide variety of scientific disciplines. Scientists have discovered important information about the ion-molecule reactions that occur in the earth's atmosphere (3) and in interstellar space (4). GPIC research has helped in the development of highly sensitive methods for chemical analysis, and in the evolution of useful theoretical methods for calculating and predicting chemical reactivity (5).

Nearly all of the instrumental techniques used to study GPIC employ a mass spectrometer (MS) for detection and measurement of ions. Among the most widely used of the MS-based techniques are ion cyclotron resonance (ICR), flowing afterglow (FA), selected ion flow tube (SIFT), time-of-flight (TOF), and pulsed e-beam high pressure mass spectrometric (PHPMS) methods. Because of the nature of ion containment and detection in a mass spectrometer, the above methods require that ionic reactions be studied at relatively low total pressures; ICR operates at 10^{-5} - 10^{-6} torr, while the other methods require pressures between 0.5 and 6 torr (6). Instrumental difficulties have for the most part prevented investigations above these pressures. However, in several recent articles (6-13), Grimsrud et al. have reported initial studies of GPIC at atmospheric pressure. The most important reason for undertaking research at atmospheric pressure was the need to understand GPIC under all physical conditions in which reactions occur.

The importance of measurements over a wide range of pressures is illustrated by the simple bimolecular nucleophilic displacement (S_N2) reaction shown below.



This reaction has been studied by ICR at about 10^{-6} torr

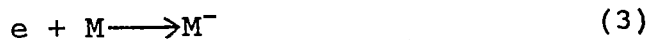
(5), by PHPMS (14), FA (15) and SIFT (16) at about 1 torr, and by kinetic ion mobility mass spectrometry (KIMMS) (6) at 640 torr. The rate constant for Reaction 1 at 300 K varies from $1.2 \times 10^{-11} \text{ cm}^3 \text{ s}^{-1}$ by ICR to 2.3, 2.1, and $2.7 \times 10^{-11} \text{ cm}^3 \text{ s}^{-1}$ by PHPMS, FA, and SIFT, respectively. At 400 K, the rate constant measured by PHPMS is $8.8 \times 10^{-12} \text{ cm}^3 \text{ s}^{-1}$ and by KIMMS it is $3.4 \times 10^{-11} \text{ cm}^3 \text{ s}^{-1}$. Riveros et al. (1), Bohme et al. (17) and Caldwell et al. (14) attribute the low value of the ICR measurement at 300 K to the large difference in pressure between ICR and the measurements at near 1 torr. The same conclusion was drawn by Giles and Grimsrud (6) with respect to the PHPMS and KIMMS measurements at 400 K. For systems like Reaction 1, changes in pressure are thought to have a significant effect on reaction dynamics. For other systems, like the analogous S_N2 reaction between Cl^- and $\text{CH}_3(\text{CH}_2)_2\text{CH}_2\text{Br}$, the rate constant is thought to be relatively independent of pressure (6). Obviously, there is a need for more measurements of reaction dynamics and energetics at much higher pressures so that scientists can gain a more complete understanding of GPIC.

The PDM-ECD

In 1988, Mock and Grimsrud introduced the photodetachment-modulated pulsed electron capture detector

(PDM-ECD), and demonstrated its utility for the trace analysis of halocarbon mixtures (18). In subsequent reports, it was shown that the PDM-ECD could be used for the study at atmospheric pressure of many GPIC processes. The PD spectra of the radical anions of 31 nitroaromatic compounds were reported for the first time (10), along with the PD spectra of the radical anions of azulene (11), SF₆ and several perfluorinated compounds (12). In some cases, these spectra were compared with the known condensed-phase absorption spectra of the anions and found to be quite similar. The instrument was shown to be useful for kinetic study when it was used to measure the thermal electron detachment rate constants for azulene (11). The PDM-ECD was also shown to be useful for determining the relative amounts of Cl⁻ and Br⁻ produced by dissociative EC from CBrCl₃ (9). Finally, experiments revealed that *p*-benzoquinone and its methylated derivatives undergo optically enhanced electron capture (OEEC) in the PDM-ECD (19, 20).

The utility of the PDM-ECD for the study of GPIC derives from several factors. First, negative ions are easily generated in the instrument by dissociative electron capture (EC), Reaction 2, or by resonance EC,



Reaction 3. A second advantage of the PDM-ECD involves the ubiquitous presence of sample impurities. In the study of many GPIC processes, such as slow ion-molecule reactions, trace contaminants can cause fast side reactions to occur that completely overwhelm the reaction of interest. As a result, researchers must take great pains to ensure the purity of their samples (6, 14-16, 21). Occasionally, simple reactions are impossible to study because of the presence of contaminants (14). Impurities are not a problem with the PDM-ECD. The instrument has a built-in "immunity" toward contaminants because "dirty" neutral reactants and negative ion precursors can be introduced to the PDM-ECD with chromatographic separation from potential impurities. A third advantage of the PDM-ECD results from its use of electron photodetachment (PD), Reaction 4, as an induced



perturbation of the ECD signal. Along with the normal EC response of the PDM-ECD, PD provides additional specificity for detection of many compounds. These compounds must capture thermalized electrons by Reaction 2 or 3, and the resulting negative ions must undergo PD by light of a chosen wavelength (22). In addition to simply providing additional response specificity, PD is a well-established method for studying negative ion

thermochemistry, spectroscopy and kinetics. Electron affinities (23-25), bond dissociation energies (26, 27), and solvation energies (28-31) have been determined by PD, along with energies of electronic transitions in negative ions (23). A final advantage of the PDM-ECD is that it operates at atmospheric pressure. In the example of the S_N2 reaction given above, research at atmospheric pressure was shown to be important to a more complete fundamental understanding of GPIC. In addition to simply increasing theoretical knowledge, research at atmospheric pressure using the PDM-ECD allows for unambiguous study of electron photodetachment spectroscopy. In the past, PD measurements have usually been made by the ICR technique. Anions formed in the ICR usually possess an excess of internal energy due to the processes by which they are formed. This excess internal energy is not removed efficiently by collisions at the operating pressures of the ICR (10^{-6} - 10^{-5} torr), and this can make the interpretation of PD spectra complicated (23). In addition, if the initially-formed excited anions possess lifetimes against autodetachment that are too short, PD cannot compete with autodetachment, because stabilizing collisions are too infrequent at the low pressure of the ICR (10). These problems are avoided in the atmospheric pressure environment of the PDM-ECD. The frequent

collisions that occur at atmospheric pressure guarantee that all species are in thermal equilibrium with one another and that negative ions will be in their ground electronic and lowest vibrational states (10).

Despite its many advantages, the PDM-ECD has several distinct drawbacks for the study of GPIC. Many negative ions of experimental interest that can be produced in other instruments cannot be generated in the PDM-ECD by resonance or dissociative EC. A related problem is that for some systems, the neutral reactants are rapidly destroyed in the PDM-ECD by one of the same two EC reactions. This limits the number of experimental systems amenable to study by the PDM-ECD.

Use of the PDM-ECD for Studies of

Gas-Phase Ion Chemistry

The past success of the PDM-ECD for a variety of investigations, along with its known advantages and disadvantages, suggest that the instrument should be useful for further study of gas-phase ion chemistry. The following work describes the utility of the PDM-ECD for detailed and fundamental investigations of GPIC. These studies are divided into three major areas: 1) quinone photochemistry, 2) iodide-water clustering equilibria, and 3) kinetics of S_N2 reactions.

The continued measurement of PD spectra for many more molecular anions is important for the reasons given above. These PDM-ECD measurements are fairly straightforward for most systems. However, in the case of the molecular anions of quinones, PD measurements are complicated by the simultaneous occurrence of optically enhanced electron capture. As it was mentioned previously, the observation of OEEC was reported recently by Mock and Grimsrud (19, 20). Further investigations using the PDM-ECD will be important to a more complete understanding of the photochemistry regarding OEEC and PD by the quinones.

Ion-molecule reactions are one area of GPIC which has not been fundamentally investigated by the PDM-ECD. In two recent reports (32, 33), Grimsrud et al. developed a second-generation version of the PDM-ECD for simple iodide- and bromide-specific detection based on PD and ion-molecule clustering. Although this early research focused on the analytical applications of clustering reactions in the PDM-ECD, the potential of the instrument for fundamental studies of a variety of ion-molecule reactions was clearly demonstrated.

Negative ion clustering equilibria are perfectly amenable to fundamental study, at atmospheric pressure by the PDM-ECD. One of the problems traditionally associated with the study of ion clustering equilibria at high

pressures is that in the measurement and detection of the clusters, the established equilibrium may be disturbed. This can be especially problematic in mass spectrometric sampling from ion sources in which the pressure exceeds about 10 torr (7, 34). The PDM-ECD should be useful for the study of negative ion clustering equilibria even though it operates at atmospheric pressure. No significant perturbation of equilibrium will occur because the measurement of ions by PD takes place within the ionization volume itself, without sampling into a region of lower pressure. For the PDM-ECD study of negative ion clustering equilibria, it is only necessary that the free and clustered anions possess distinct PD spectra. An initial study of the negative ion clustering reaction between iodide and water will be investigated by the PDM-ECD. This investigation of iodide-water clustering is important because it can provide a model for future PD studies of clustering by the PDM-ECD and by other methods.

Bimolecular nucleophilic displacement is another simple ion-molecule reaction that can be studied by the PDM-ECD. It is clear from the earlier discussion of the reaction between Cl^- and CH_3Br that there is important fundamental knowledge, especially in the area of kinetics, to be gained by the study of $\text{S}_{\text{N}}2$ reactions at atmospheric pressure. For the study of $\text{S}_{\text{N}}2$ reactions by the PDM-ECD,

all that is necessary is that the PD spectra of the reagent and product ions be distinguishable. The reactions of alkyl bromides with chloride are well-suited for this type of study by the PDM-ECD. The PD spectra of Cl^- and Br^- are different, and the reactions between Cl^- and a few alkyl bromides have recently been characterized by other methods (6, 14, 16).

THEORY

Collision Frequency and ThermalizationWithin the PDM-ECD

As it was discussed in the Introduction, the dynamics of gas-phase processes near atmospheric pressure differ significantly from those at lower pressures. For a thorough understanding of the PDM-ECD, it is therefore important to predict how increased pressure will affect gas-phase ion chemistry.

The fundamental difference between GPIC at atmospheric pressure and at lower pressures has to do with collision frequency, z . The value for z at a particular pressure may be calculated from Equation 5, where \bar{v} is the

$$z = \bar{v}\sigma\sqrt{2}\frac{N}{V} \quad (5)$$

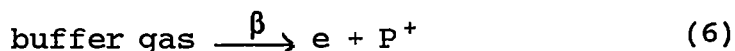
mean velocity of the particles and N/V is their number density. The term, σ , is the collision cross-section and is calculated from $\sigma = 2\pi r^2$ where r is the radius of the particles (35). Using this equation, the calculated collision frequency at 640 torr and 125°C is $\sim 7 \times 10^9 \text{ sec}^{-1}$. GPIC is often studied in the one torr range by PHPMS and FA methods, and by ICR at 10^{-5} torr. At one

torr the value for z is smaller than at atmospheric pressure by about three orders of magnitude, while in the 10^{-5} torr ICR cavity, z is incredibly low, $\sim 100 \text{ sec}^{-1}$.

The most important result of the high collision frequency at atmospheric pressure is that excited ions and molecules are rapidly stabilized and brought into thermal equilibrium with the buffer gas (36). As it was mentioned in the Introduction, this is important because ionization processes and energetic ion-molecule reactions often produce excited species that contain substantial internal energy. Meot-Ner concluded that for a variety of ion/buffer gas systems, vibrationally excited ions are generally thermalized in about 10 collisions, and a Boltzmann temperature distribution is attained after about 100 collisions (37). Therefore, from the collision frequencies determined above, collisional stabilization at atmospheric pressure takes place in about 1 nsec, which easily allows for the thermal study of even the fastest ionic reactions.

Reactions Within the Cell

The production of ions in the PDM-ECD cell volume begins with Reaction 6, in which the buffer gas is ionized



by beta particles emitted from a ^{63}Ni -on-Pt foil. The rate constant for this reaction is β . The foil used has an activity, A , of 8 mCi (3×10^8 disint sec^{-1}), and the average energy of a beta particle, E_β , is 17 keV. Using these numbers, a value of $\beta = 7 \times 10^{10}$ ion pairs sec^{-1} is calculated from Equation 7, where 35 eV is the amount of

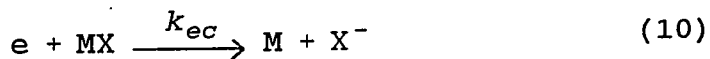
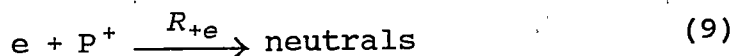
$$\beta = \frac{\frac{1}{2} AE_\beta}{35\text{eV}} \quad (7)$$

energy required from the beta particle to produce one ion pair. The average electron density in the cell, $[e]$, can then be calculated from Equation 8, where V_o is the cell

$$[e] = \sqrt{\frac{\beta}{V_o R_{+e}}} \quad (8)$$

volume and the positive ion-electron recombination rate constant is given by $R_{+e} = 3 \times 10^{-6} \text{ cm}^3 \text{ sec}^{-1}$ (38). With a 2.65 cm^3 cell volume, the electron density is calculated to be $9 \times 10^7 \text{ cm}^{-3}$. The electron density in the cell is continuously monitored by collecting the electrons at positively-charged pin that is pulsed at a fixed frequency.

Once formed, the thermal electrons can interact with species present in the cell by Reactions 9-11.

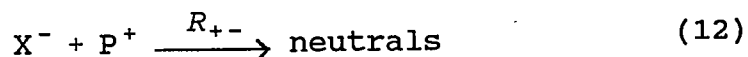


The recombination of positive ions with electrons is shown in Reaction 9. The pseudo first-order rate constant, R_{+e} , is calculated from the above values to be 270 sec^{-1} .

Reactions 10 and 11 are dissociative and resonance electron capture, respectively. One of these reactions will occur when a molecule with a high electron affinity enters the cell. Dissociative electron capture leads to formation of an atomic negative ion, while resonance electron capture forms the molecular anion. In the case of resonance electron capture, it is important to note that the reaction is actually a two step process. First, the molecule captures an electron to form the excited molecular anion, M^{-*} . In order to form a stable molecular anion, this species then undergoes a rapid series of collisions with the buffer gas (as described in the previous section) which collisionally stabilize the anion and bring it into thermal equilibrium with the other gas molecules. Electron capture (EC) by either the dissociative or resonance method causes a decrease in the

average electron density within the cell, and a concomitant decrease in the monitored response at the positively pulsed pin.

Negative ions are destroyed by Reactions 12 and 13.

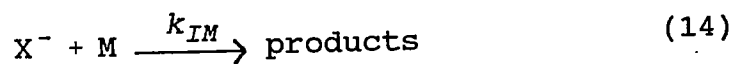


In the absence of light, negative ions will be lost almost exclusively by ion-ion recombination, Reaction 12. Although a few ions are also lost by diffusion to the walls, Zook (36) determined that the first-order rate constant for this process is only about 5 sec^{-1} for a cell of similar size. Ventilation of ions from the cell is also insignificant in the PDM-ECD, as the value is less than 1 sec^{-1} . $R_{+-}[P^+]$ is the pseudo first-order rate constant for ion-ion recombination. The value for $R_{+-}[P^+]$ has been estimated by Mock and Grimsrud (18) to be equal to $100 \pm 50 \text{ sec}^{-1}$ for the PDM-ECD instrument. It is thought to be independent of the identity of the EC-active species (18) and independent of temperature (11).

If a negative ion is formed during irradiation of the cell, electron photodetachment (PD), Reaction 13, may occur. For this reaction to take place, the photon energy must be greater than the electron affinity of the

corresponding neutral. Reaction 13 returns a bound electron to the continuum, to be collected at the pin. The original electron capture event is therefore not detected by the instrument if Reaction 13 occurs. The pseudo first-order rate constant, k_{hv} , depends on the photon flux through the cell and on the PD cross-section of the negative ion. Even though the experimental values for k_{hv} are smaller than $R_{+}[P+]$, Mock and Grimsrud found that they could easily monitor PD by passing a chopped light beam through the cell and measuring the resulting perturbation by the method described in Experimental (18).

Before it is destroyed, a negative ion can react with a neutral in the PDM-ECD and undergo an ion-molecule reaction, as shown in Reaction 14. In this type of



reaction, the products might be species such as clustered ions or exchange products. In many reactions of this type, products are formed at nearly every collision between the ion and the neutral. These reactions are said to be collisionally limited. The Langevin/ADO collision rate constant, k_c , corresponds to this second-order process of unit efficiency. It has a value of about 10^{-9} $\text{cm}^3 \text{sec}^{-1}$, and can be calculated for a specific system

from Equation 15 (39) with parameters from several sources (39-41).

$$k_c = \frac{2\pi q}{\mu^{\frac{1}{2}}} \left[\alpha^{\frac{1}{2}} + c\mu_D \left(\frac{2}{\pi KT} \right)^{\frac{1}{2}} \right] \quad (15)$$

q = charge = 4.8×10^{-10} esu
 μ = reduced mass
 α = polarizability of molecule (ref. 41)
c = dipole locking constant (ref. 39)
K = Boltzmann's constant = 1.38×10^{-16} erg
T = absolute temperature = 398 K

Equilibrium Within the PDM-ECD

Kebarle has listed three criteria that are necessary for the establishment of ionic equilibrium in the gas phase. First, the reactants must be in thermal equilibrium with the surroundings. Second, the ions that are involved in the equilibrium must be coupled by reactions that are faster than all other processes that affect their concentrations. Third, the system must be allowed enough time to reach equilibrium (42).

The three criteria listed above are met in the PDM-ECD. In a previous section, it was demonstrated that thermalization readily occurs at atmospheric pressure in the PDM-ECD ionization volume. Krieger and Grimsrud have shown that at atmospheric pressure, equilibrium is attained extremely quickly in comparison with the

competing processes of ion-ion recombination, ventilation from the cell and diffusion (43). Finally, in the PDM-ECD, the pulsing of the pin is responsible for collecting the electrons in the cell and monitoring the course of ionic reactions. The typical pulsing period of 200 μ s is far longer than the lifetime of an ion (43) involved in a typical gas-phase ionic reaction at equilibrium.

EXPERIMENTAL

PDM-ECD Setup

A schematic representation of the PDM-ECD setup is shown in Figure 1. The following sections describe the experimental considerations associated with each aspect of the system.

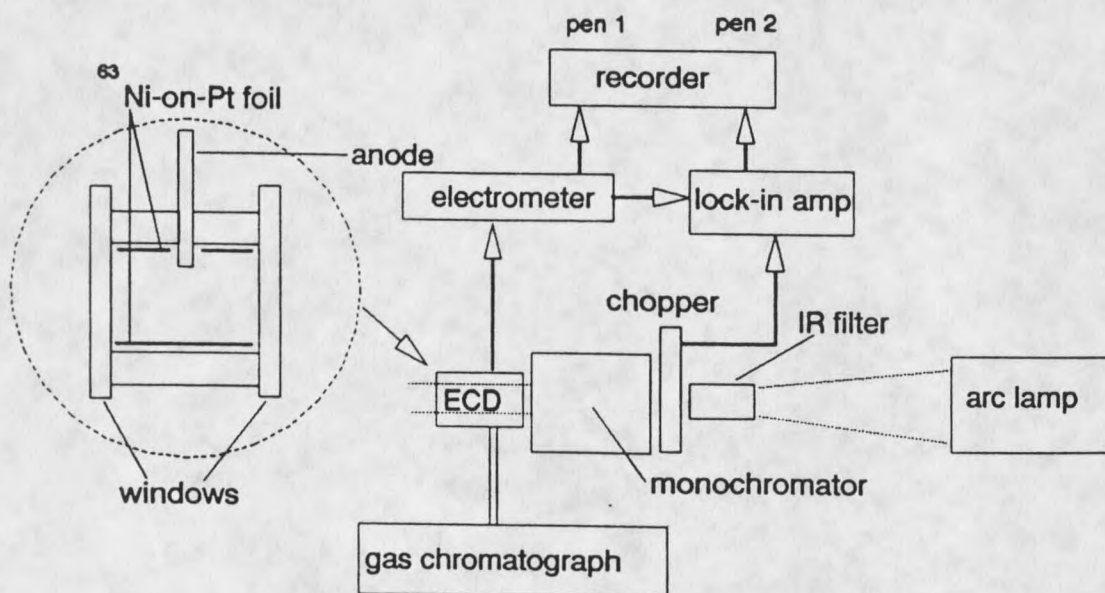


Figure 1. Apparatus used for PDM-ECD studies.

The ECD

The ECD was constructed from a solid block of stainless steel with a central cylindrical cavity. The walls of the cavity were formed by a ^{63}Ni -on-Pt foil of 9 mCi activity. The cavity was 2.0 cm long and 1.3 cm wide, which resulted in an ionization volume of 2.65 cm³. Fused silica windows form the front and rear walls of the cavity and allow for light to enter the ionization volume. They were sealed with teflon washers. The external transmittance of these windows reaches 90% at 220 nm and remains constant until nearly 1.5 μ . The operating temperature range of the ECD was from room temperature to 200°C. The temperature was regulated by a Watlow temperature controller equipped with two cartridge heaters and a thermocouple feedback control. A stainless steel pin with a diameter of $1/16$ in. served as the anode. It entered the ECD from the side through a teflon plug and protruded $1/8$ in. into the ionization volume. The pressure within the ECD was approximately 640 torr (atmospheric pressure in Bozeman) for all experiments.

Sample Introduction

The halocarbons and quinones were obtained from commercial suppliers and were used without further purification since the GC provided adequate separation of

the desired compounds from any potential impurities. For small halocarbons with boiling points less than about 80°C, gas samples were prepared in nitrogen by successive dilution into gas-tight glass vessels. A 4.3 L glass carboy was pressurized to 1150 torr and was used for final storage of the samples. This method allowed numerous aliquots to be transferred by a 30 mL gas-tight syringe to the gas sampling loop. The reproducibility of sample delivery by this method is very good (less than 5% variation) (44). The larger halocarbons were diluted in HPLC-grade hexane to achieve an appropriate concentration. The quinones were diluted in HPLC-grade toluene. Between 0.1 μ L and 1 μ L of these liquid samples were injected onto the GC with a 1 μ L syringe.

Samples were introduced into the PDM-ECD upon elution from a gas chromatograph (GC) (Varian Model 3700). Three different columns and two different injection methods were used. The gaseous samples were introduced to the gas chromatograph by a 2.0 cm³ gas sampling loop (Carle Model 8030). The stainless steel column used was 10-ft \times 1/8 in. and was packed with 10% SF-96 on Chromosorb W. For the quinones and the larger halocarbons with boiling points above 80°C, the liquid samples were introduced to the GC by a heated direct on-column injection port. A wide-bore 3 meter capillary column (Hewlett Packard HP-17:

50% phenyl- and 50% methyl polysiloxane) was used for the quinones. A megabore 15 meter capillary column (Alltech RSL-200: polydiphenyldimethylsiloxane) was used for the larger halocarbons. The carrier and make-up gases were 10% methane in argon for the halocarbons and nitrogen for the quinones. The gases were purified by passage through water- and oxygen-removing traps (Alltech). The flow rates of the carrier and make-up gases were measured separately and were varied along with the column temperature to achieve optimal separation, retention time and chromatographic peak shape for each compound. The chromatographic retention times of all compounds were determined from parallel GC studies with flame ionization detection and/or mass spectrometric detection.

Calculation of Sample Concentration

Within the ECD

For many of the compounds studied, it was necessary to know the concentration of the analyte within the ECD at the time corresponding to the maximum of the chromatographic peak. The calculation of this quantity is facilitated by the gaussian shape of most of the chromatographic peaks. It is well-known that 95.5% of the area of a gaussian peak is contained within 2σ on either side of the maximum (45). It is also known that a triangle drawn with two sides tangent to the inflection

points on the sides of a gaussian peak will intersect the base exactly 2σ on either side of the maximum (46) (see Figure 2). It is therefore easy to locate on a chromatogram the points on the baseline that correspond to -2σ and $+2\sigma$. If a chromatographic peak is gaussian in shape, 95.5% of the analyte mass will have eluted during the time corresponding to 4σ . For a gaussian peak of area = 1, the average magnitude of the curve, \bar{y} , will be given by $0.955/4 = 0.239$, as shown in Figure 2. For a chromatographic peak, the average concentration (in molec mL^{-1}) of the analyte within the ECD, \bar{c} , can be calculated from Equation 16, where # is the number of molecules

$$\bar{c} = \# / WF \quad (16)$$

injected, W is the time width of the base of the triangle as shown in Figure 2, and F is the flow rate in mL sec^{-1} . The magnitude of a gaussian peak at its maximum is 0.3989 (45), and is a factor of 1.67 greater than \bar{y} . Therefore, multiplication of \bar{c} by 1.67 gives the concentration of the analyte within the ECD at the time corresponding to the maximum of the chromatographic peak.

Doping of the Make-up Gas

For the iodide-water clustering experiments, it was necessary to introduce a known partial pressure of water into the ionization volume. This was accomplished by inserting a glass bubbling device into the make-up gas

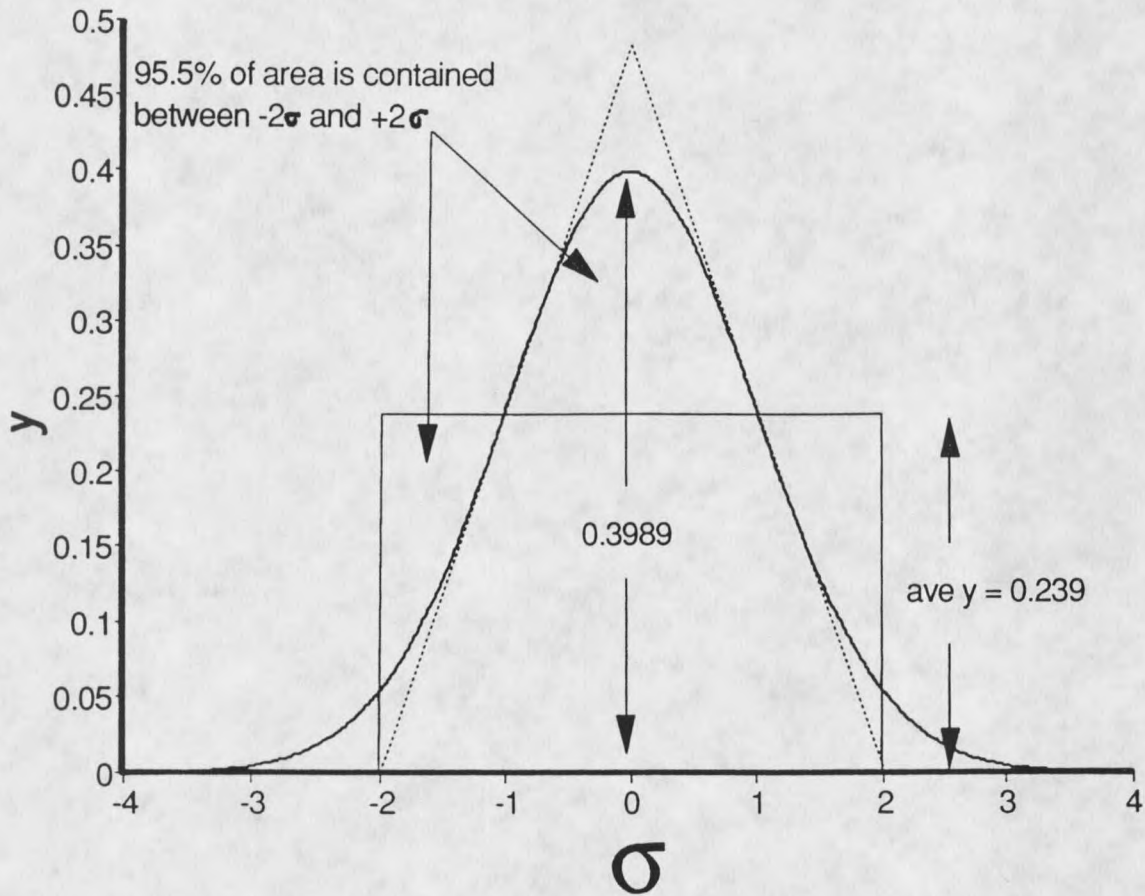


Figure 2.

A gaussian peak of unit area is represented by the solid line. The dashed lines are drawn tangent to the inflection points of the sides of the peak and intersect the x-axis at exactly -2σ and $+2\sigma$. 95.5% of the total area under a gaussian peak is contained between -2σ and $+2\sigma$. The average value for the magnitude of the gaussian curve between -2σ and $+2\sigma$ is 0.239. For a gaussian peak of unit area, the value at the peak maximum is 0.3989.

line after the oxygen- and water-removing traps. The setup of the bubbler in conjunction with the GC is shown in Figure 3. Make-up gas was bubbled through a fritted glass inlet into the enclosed vessel, which contained HPLC-grade water. The bubbler was immersed in a temperature controlled water bath. The water-saturated make-up gas passed through heated transfer lines and was mixed with the effluent from the GC immediately prior to the PDM-ECD. The partial pressure of water in the PDM-ECD was calculated from the temperature of the bubbler and the ratio of make-up gas flow to total flow through the PDM-ECD.

For the S_N2 experiments, it was necessary to introduce a compound to the PDM-ECD that produced unclustered chloride ion following dissociative electron capture in the ionization volume. CF_2Cl_2 (Matheson) was introduced into the PDM-ECD as shown in Figure 3. With an extremely slow flow rate, the compound was introduced continually into the make-up gas line through a needle valve. The introduction of CF_2Cl_2 was controlled so that the normal ECD current (described in Signal Processing) was reduced to half of its undoped value. Under these conditions, the chloride concentration was thought to be approximately equal to that of electrons in the ionization volume.

